Loss of Proteostasis Is a Pathomechanism in Cockayne Syndrome

Article *in* Cell Reports · May 2018
DOI: 10.1016/j.celrep.2018.04.041

12 authors, including:

Alupei Marius Costel
Ulm University
16 PUBLICATIONS **93** CITATIONS
SEE PROFILE

Philipp Ralf Eßer
University Medical Center Freiburg
57 PUBLICATIONS **1,019** CITATIONS
SEE PROFILE

Ioanna Krikki
Ulm University
14 PUBLICATIONS **3** CITATIONS
SEE PROFILE

Francesca Tuorto
German Cancer Research Center
53 PUBLICATIONS **2,294** CITATIONS
SEE PROFILE

Cell Reports

Loss of Proteostasis Is a Pathomechanism in Cockayne Syndrome

Graphical Abstract

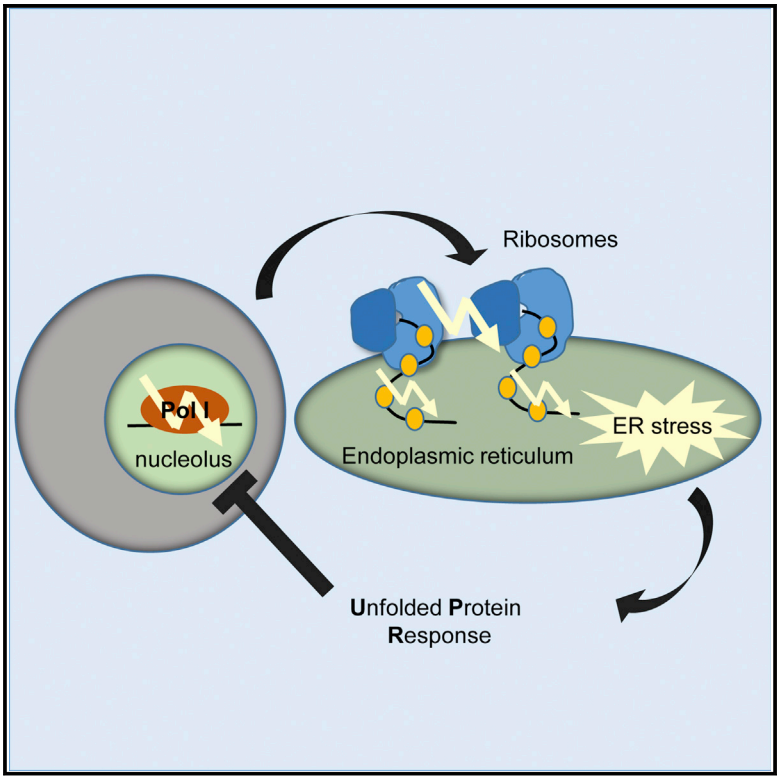

Authors

Marius Costel Alupei, Pallab Maity, Philipp Ralf Esser, ..., Lorenzo Montanaro, Karin Scharffetter-Kochanek, Sebastian Iben

Correspondence

sebastian.iben@uni-ulm.de

In Brief

Cockayne syndrome is a devastating childhood progeria. Here, Alupei et al. show that cells from CS patients have reduced translation accuracy and elevated ROS, leading to generation of unstable proteins and activation of ER stress. Reducing ER stress by chemical chaperones in these cells rescues RNA polymerase I activity and protein synthesis.

Highlights

- Cockayne syndrome cells show reduced translation fidelity
- Elevated oxidative stress and misfolded proteins activate the unfolded protein response
- The unfolded protein response suppresses Pol I activity in CS cells
- Chemical chaperones alleviate ER stress and restore Pol activity in CS cells

Alupei et al., 2018, Cell Reports *23*, 1612–1619
May 8, 2018
https://doi.org/10.1016/j.celrep.2018.04.041

CellPress

OPEN ACCESS
CellPress

Cell Reports
Report

Loss of Proteostasis Is a Pathomechanism in Cockayne Syndrome

Marius Costel Alupei,[1] Pallab Maity,[1] Philipp Ralf Esser,[2] Ioanna Krikki,[1] Francesca Tuorto,[3] Rosanna Parlato,[4,5] Marianna Penzo,[6] Adrian Schelling,[1] Vincent Laugel,[7] Lorenzo Montanaro,[6] Karin Scharffetter-Kochanek,[1] and Sebastian Iben[1,8,*]

[1]Clinic of Dermatology and Allergic Diseases, University Medical Center, Albert-Einstein Allee 23, 89081 Ulm, Germany
[2]Allergy Research Group, Department of Dermatology, University Medical Center Freiburg, Faculty of Medicine, 79104 Freiburg, Germany
[3]Division of Epigenetics, DKFZ-ZMBH Alliance, German Cancer Research Center, 69120 Heidelberg, Germany
[4]Institute of Applied Physiology, Ulm University, 89081 Ulm, Germany
[5]Institute of Anatomy and Medical Cell Biology, Heidelberg University, 69120 Heidelberg, Germany
[6]Laboratorio di Patologia Clinica, Dipartimento di Medicina Specialistica, Diagnostica e Sperimentale, Università di Bologna, Via Massarenti 9, 40138 Bologna, Italy
[7]Laboratoire de Génétique Médicale - INSERM U1112, Institut de Génétique Médicale d'Alsace (IGMA), Faculté de médecine de Strasbourg, 11 rue Humann, 67000 Strasbourg, France
[8]Lead Contact
*Correspondence: sebastian.iben@uni-ulm.de
https://doi.org/10.1016/j.celrep.2018.04.041

SUMMARY

Retarded growth and neurodegeneration are hallmarks of the premature aging disease Cockayne syndrome (CS). Cockayne syndrome proteins take part in the key step of ribosomal biogenesis, transcription of RNA polymerase I. Here, we identify a mechanism originating from a disturbed RNA polymerase I transcription that impacts translational fidelity of the ribosomes and consequently produces misfolded proteins. In cells from CS patients, the misfolded proteins are oxidized by the elevated reactive oxygen species (ROS) and provoke an unfolded protein response that represses RNA polymerase I transcription. This pathomechanism can be disrupted by the addition of pharmacological chaperones, suggesting a treatment strategy for CS. Additionally, this loss of proteostasis was not observed in mouse models of CS.

INTRODUCTION

Recessive mutations in genes encoding five different DNA repair proteins (CSA, CSB, XPB, XPD, XPG) of the nucleotide-excision repair (NER) pathway can cause the premature aging disorder Cockayne syndrome (CS), characterized by neurological degeneration, cataracts, alopecia, and severe growth failure ("cachectic dwarfs") with a median life expectancy of 12 years (Laugel et al., 2010).

CS is characterized by the failure of a sub-pathway of NER, hence CS is mainly regarded as a DNA-repair disease. Because the total loss of NER is not necessarily followed by developmental impairment and premature aging, alternative concepts are also under investigation (Brooks, 2013).

All CS proteins participate in a key step of ribosomal biogenesis, the transcription by RNA polymerase I in the nucleolus (Bradsher et al., 2002; Iben et al., 2002; Koch et al., 2014; Schmitz et al., 2009). The CS proteins XPB and XPD, which are part of the basal RNA polymerase I and II transcription factor TFIIH, enhance elongation of RNA polymerase I (Assfalg et al., 2012; Nonnekens et al., 2013). The CSA factor stimulates re-initiation of RNA polymerase I transcription and recruitment of the elongation factors CSB and TFIIH to the rDNA promoter (Koch et al., 2014). Mutations in these factors disturb RNA polymerase I transcription *in vitro* and *in vivo* (Assfalg et al., 2012; Bradsher et al., 2002; Koch et al., 2014; Lebedev et al., 2008). A null mutation in *CSB* was identified in a UV-sensitive (UVs) patient with a DNA repair defect but a mild, sun-sensitive skin disease (Horibata et al., 2004) without the severe developmental symptoms of Cockayne patients. UVs syndrome can also be caused by mutations in CSA and CSB. However, CS cells are, in contrast to UVs syndrome cells, hypersensitive to oxidizing agents, a feature that might contribute to or even cause developmental delay and premature aging.

The mouse models of CS with Csb or Csa mutations display mild phenotypes without the dramatic growth retardation or shortage of lifespan (van der Horst et al., 1997, 2002).

In this study, we used patient-derived cell lines and as control, the respective cells reconstituted with the wild-type gene. All results were additionally controlled using cells from a non-progeroid UVs-syndrome patient. Knowing that all CS mutations affect ribosomal biogenesis, we asked what are the cellular consequences of a disturbed RNA polymerase I transcription. A failure in RNA polymerase I transcription can influence the stability of the proteome and, in combination with the elevated reactive oxygen species (ROS) found in CS cells, could induce an unfolded protein response, consequently repressing RNA polymerase I

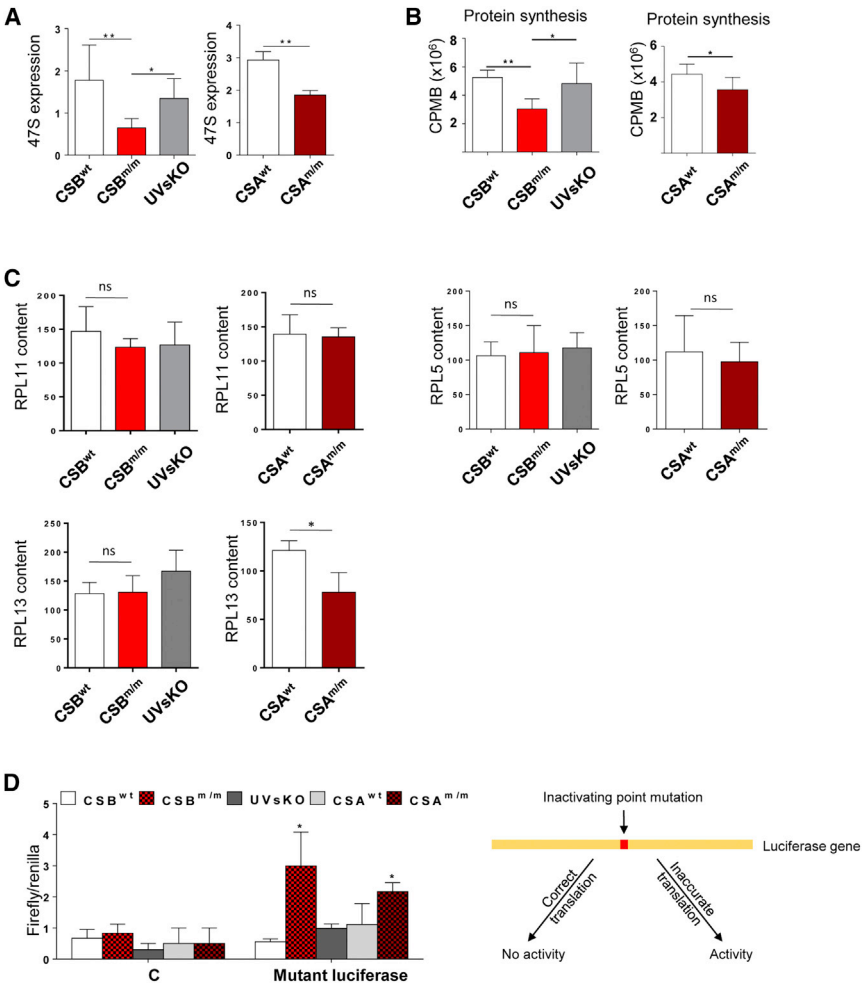

Figure 1. Deficient RNA Pol I Activity and Protein Translation

(A) Analysis of precursor 47S rRNA expression by qPCR in CSB- and CSA-deficient cells. The values were normalized to RPL13 expression. Values are mean ± SD of three independent experiments (*$p < 0.05$, **$p < 0.01$).

(B) Metabolic labeling of CS and control cells for 2 hr with ^{35}S methionine/cysteine, indicating the rate of total protein synthesis.

(C) Quantification of ribosomal content by western blot analysis of RPL11, RPL13, and RPL5 levels from isolated ribosomes from CS and control cells. Values are mean ± SD of three independent experiments.

(D) Translation accuracy was measured in CS and control cells by transfection of control or mutant firefly luciferase reporters, with a mutated critical lysine 529, determining the frequency of amino acid misincorporation. The principle of the assay is depicted in the scheme below. The activity of the luciferase was determined by luminescence measurement and normalized to the luminescence of *Renilla* luciferase. Values are mean ± SD of three independent experiments (*$p < 0.05$).

transcription. Here, we provide evidence that this mechanism is present in CS cells, and we show that it can be disrupted by treatment with pharmacological chaperones, indicating a treatment opportunity for CS children.

RESULTS

RNA Polymerase I Transcription and Protein Translation Are Affected in CS Cells

We used established patient-derived cell lines with mutations in CSB (CS1AN) (Troelstra et al., 1992), CSA (CS3BE) (Henning et al., 1995), a CSB null mutation without the clinical severity of Cockayne syndrome (UVsKO) (Horibata et al., 2004), and the wild-type-reconstituted counterparts to investigate transcription and translation.

Using qPCR, we showed that the rate of 47S pre-rRNA precursor transcription in cells of CS patients ($CSB^{m/m}$, $CSA^{m/m}$) is strongly reduced in comparison to control cells (reconstituted CSB^{wt}, CSA^{wt}, or cells from CSB null UVs patient, UVsKO) (Figure 1A). Next, using metabolic labeling and flow cytometry we found that protein translation was significantly reduced in CS cells (Figures 1B and S1A). These cells, however, contain the same amount of ribosomes as the control cells, measured after sucrose-cushion centrifugation and western blotting for ribosomal proteins (Figure 1C). Hence, the decreased protein translation per ribosome in CS cells could suggest a malfunction of the translational machinery. Polysomal profiling of the ribosomes identified a reduction of the polysome to ribosome ratio in CSA mutant cells, but not in CSB mutant cells (Figure S1B).

To further address the impact on the quality of protein translation in CS cells, we investigated translational fidelity using a luciferase-based assay (Azpurua et al., 2013). As demonstrated in Figure 1D, erroneous incorporation of the right amino acid in the active center of luciferase is significantly higher in CS cells compared to controls. This result shows that a qualitative disturbance of the ribosomes in terms of translational fidelity is detectable in cells from CS patients. Transcriptional and post-transcriptional changes of rRNA could be responsible for disturbances of translation accuracy. However, RNA sequencing (RNA-seq) analysis did not reveal an increased variation frequency in rRNA of CS cells. The accession number for the rRNA sequences reported in this paper is NCBI Sequence Read Archive (SRA): SUB3922352. Additionally, rRNA pseudouridylation was similar in CS and control cells lines (Figures S1C and S1D). Future studies including *in vitro* translation analysis will unravel the molecular base of the translational inaccuracy.

Misfolded Proteins and Elevated ROS in CS Cells

Inaccurate translation could yield misfolded proteins that are susceptible to unfolding in the presence of chaotropic reagents

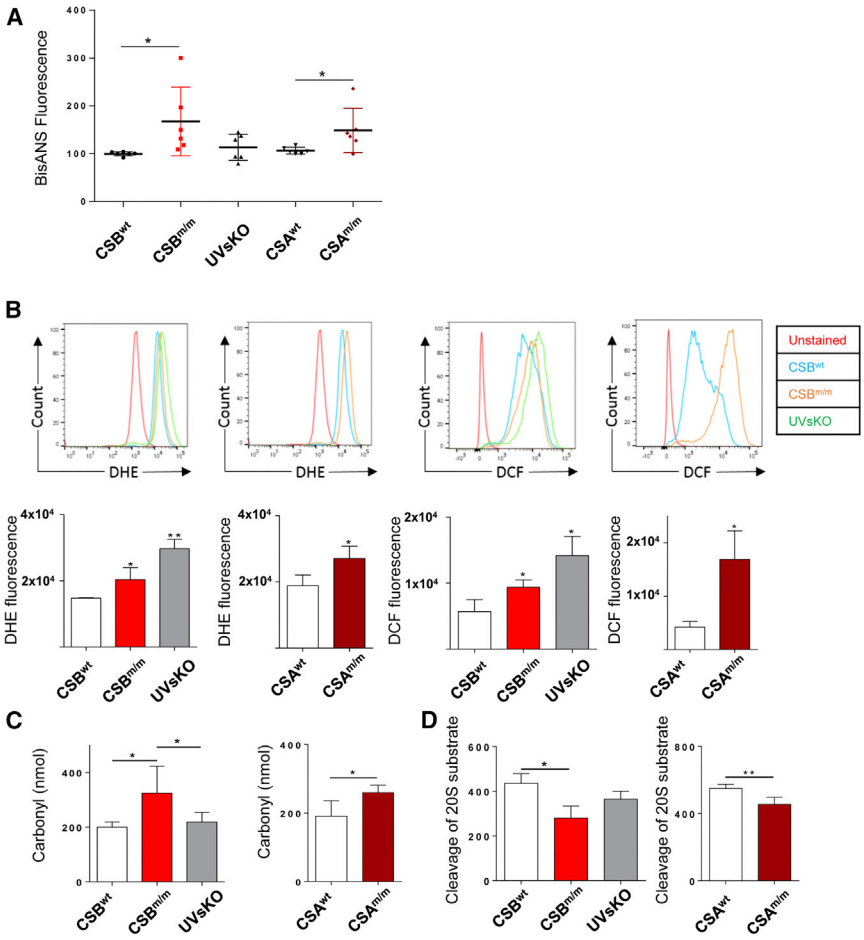

Figure 2. ER Stress in CS Cells and Sensitivity to ER Stress-Inducing Agents

(A) Protein stability was measured after denaturation with 2 M urea (2 hr) and labeling with BisANS fluorescent dye. Fluorescence intensity of BisANS was measured at 500 nm after excitation at 375 nm. The data show the percentage of BisANS fluorescence increase in CS cells, after normalizing to control cells (100% fluorescence). Values are mean ± SD of four independent experiments (*$p < 0.05$).

(B) Intracellular ROS levels assessed by DHE (left) and DCFH (right) oxidation-sensitive fluorescent dyes in CS cells. Fluorescence values were detected by flow cytometry and reported values are means of three independent experiments ± SD (*$p < 0.05$, **$p < 0.01$).

(C) Oxidation of proteins determined by the amount of carbonyl groups in CS and control cells, detected by absorbance of DNPH-tagged proteins. Values are mean ± SD of three independent experiments (*$p < 0.05$).

(D) Proteasome activity was measured in CS and control cells. Cell lysates from each group were incubate with a 20S Substrate (SUC-LLVY_AMC), and the fluorescence of the cleaved substrate was measured (360 nm excitation and 480 nm emission). Values are mean ± SD of three independent experiments (*$p < 0.05$, **$p < 0.01$).

(Pérez et al., 2009). Treating extracts of CS and control cells with 2 M urea and measuring the incorporation of a fluorescent dye (BisANS) in exposed hydrophobic domains revealed that the proteomes of CS cells displayed a higher susceptibility to protein unfolding (Figure 2A). As misfolded proteins are prone to oxidation by the elevated ROS in CS cells (Pascucci et al., 2012), we determined ROS levels in CS and control cells. Using the fluorescent dyes dihydroethidium (DHE) and dichlorofluorescein diacetate (DCF), we measured superoxide anions (O_2^-) and hydrogen peroxide (H_2O_2) levels by flow cytometry (Cleaver et al., 2014). Both CSA and CSB mutant cells showed increased amounts of O_2^- and H_2O_2 compared to control cells (Figure 2C), indicating a high level of oxidative stress. Interestingly, cells from the mildly affected UVs syndrome patient without CSB protein showed the highest ROS levels.

Hence, we hypothesized that reduced translational fidelity render CS cells more prone to oxidative protein damage. To address this hypothesis, we quantitated protein carbonylation in CS cells by dinitrophenylhydrazine (DNPH) tagging of carbonyl groups, as carbonyl presence is a direct indicator of protein oxidation. As shown in Figure 2C, protein carbonylation is increased in CS cells compared to control cells. Moreover, protein carbonylation was not elevated in the cell line with the highest load of ROS from the UVs patient (UVsKO), indicating that susceptible protein products are required for elevated oxidative protein damage.

Analysis of proteasome activity in CS cells revealed a significant reduction of protein degradation in CS cells (Figures 2D and S2A). Therefore, the decreased protein synthesis could be balanced by a decreased protein degradation. Additional experiments revealed that inhibition of rRNA transcription influences proteasomal activity (Figures S2B and S2C).

Endoplasmic Reticulum Stress in CS Cells Impairs RNA Polymerase I Transcription and Can Be Alleviated by Pharmacological Chaperones

Oxidative stress and the presence of misfolded and carbonylated proteins generate endoplasmic reticulum (ER) stress and activate the unfolded protein response (UPR) (Martínez et al., 2017).

The ER stress marker GRP78 was elevated in CS cells (Figures 3A and S3B). GRP78 elevation activates the PERK pathway, resulting in phosphorylation of the translation-initiation factor eIF2α. As we show in Figure 3A, eIF2α was strongly phosphorylated in CS cells but not in control cells, indicating an ER stress induction (Figure S3B).

To investigate if CS cells are hypersensitive to ER stress, we treated CS and control cells with tunicamycin that blocks N-glycosylation of proteins and provokes ER stress and UPR. In Figure 3B, we showed that tunicamycin specifically induced apoptosis in CS cells, which could be partially (CSB) or completely (CSA) rescued by the pre-treatment of cells with

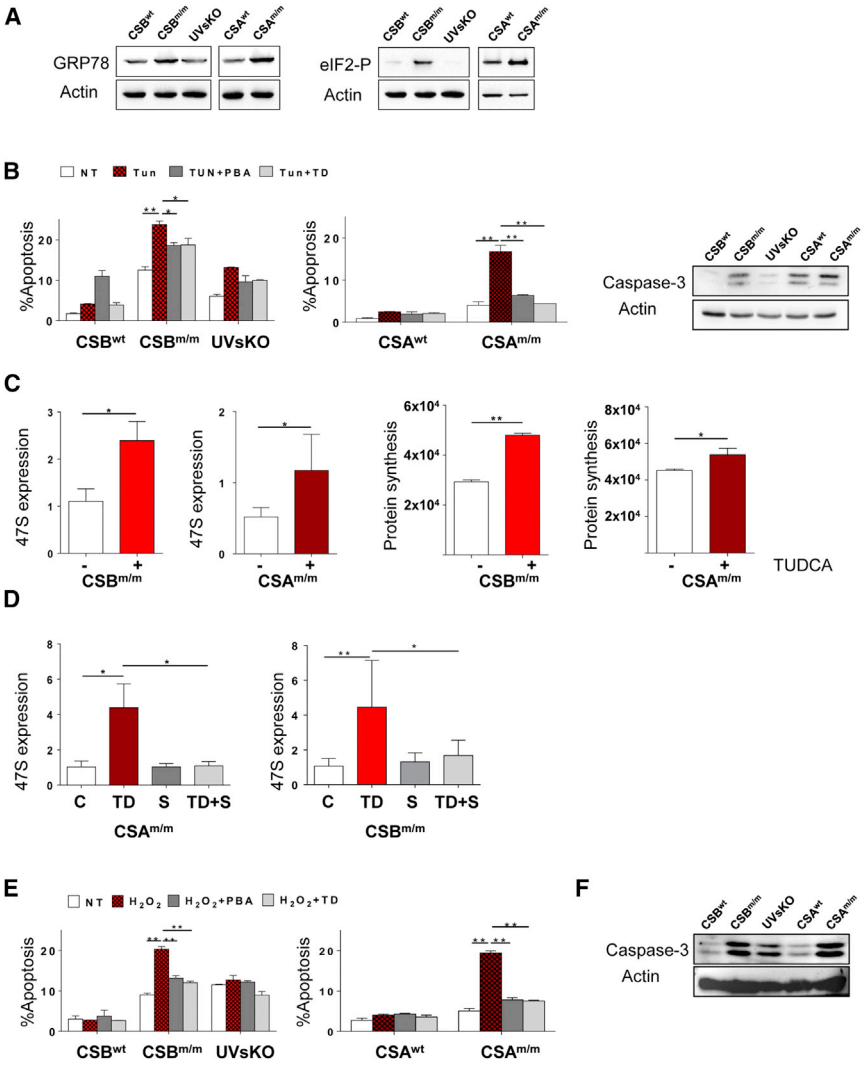

Figure 3. Chemical Chaperones Improve Translation and Prevent Oxidative Stress-Mediated Cell Death

(A) GRP78 and p-eIF2α expression were determined from whole cell lysates of CS and control cells, using western blot analysis. β-actin (lower band) was used as loading control. Three independent experiments were performed and the expression was quantified and normalized to β-actin (SI2).

(B) Resistance of CS and control cells to ER stress-mediated cell death was determined by PI staining (Nicoletti assay) and by cleaved Caspase-3 assessment using western blot. For Nicoletti assay, cells were incubated with either tunicamycin (Tun) alone (5 μg/mL) for 24 hr or after preincubation with TUDCA (TD) (200 μM) and 4PBA (1 mM) to reduce ER stress. Values are mean ± SD of three independent experiments (*$p < 0.05$, **$p < 0.01$).

(C) 24-hr incubation with TUDCA (+) significantly improves Pol I activity, determined by qPCR analysis of 47S rRNA (left graphs) and total protein synthesis (right graphs). Values are mean ± SD of three independent experiments (*$p < 0.05$, **$p < 0.01$).

(D) Specificity of TUDCA (TD) treatment on Pol I activity (47S rRNA expression) was tested using 30 μM salubrinal (SAL), a p-eIF2 phosphatase inhibitor, alone or in combination with TUDCA (SAL+TD) for 24 hr. Values are mean ± SD of three independent experiments (*$p < 0.05$, **$p < 0.01$).

(E) CS and control cells sensitivity to H_2O_2-induced cell death was determined by PI staining (Nicoletti assay). Chemical chaperones TUDCA (200 μM) and 4PBA (1 mM) were preincubated 24 hr prior to H_2O_2 treatment to prevent ER stress induction. After pretreatment, cells were incubated with H_2O_2 (500 μM) for 12 hr. Values are mean ± SD of three independent experiments (*$p < 0.05$, **$p < 0.01$).

(F) Expression of cleaved Caspase-3 (upper band) was determined from whole cell lysates of CS and control cells treated with H_2O_2 (500 μM, 12 hr), using western blot analysis. β-actin (lower band) was used as loading control. Blots are representatives of at least three independent experiments.

pharmacological chaperones as 4PBA (4-phenyl butyric acid) and TUDCA (tauroursodeoxycholic acid).

We next investigated whether the reduction in RNA polymerase I transcription observed in CS cells (Figure 1A) might be due to ER stress and UPR (DuRose et al., 2009). Hence, we treated CS (Figure 3C) and control cells (Figure S1A) with the pharmacological chaperone TUDCA for 24 hr. Indeed, rRNA transcription and also protein synthesis was markedly de-repressed in CS cells after treatment with chaperones. To validate that TUDCA-dependent relief of RNA polymerase I repression is mediated by attenuation of the UPR via PERK pathway, cells were simultaneously treated with salubrinal, an inhibitor of the p-eIF2α phosphatase and with TUDCA. Salubrinal blocked the de-repressive effect of TUDCA on RNA polymerase I transcription in CS cells, indicating that the repression is due to eIF2α phosphorylation and protein misfolding, as shown in Figure 3D.

Cells from the severe progeroid Cockayne syndrome and the mildly affected UVs syndrome differ in their hypersensitivity to oxidative stress. To test whether the hypersensitivity is mediated by the UPR, we pre-treated CS and control cells with pharmacological chaperones before the addition of H_2O_2. In Figure 3E, we could clearly show that pre-treatment of CS cells with chaperones completely prevented apoptosis following H_2O_2 challenge, whereas basal apoptosis levels were not influenced by TUDCA treatment (Figure S3C). Apoptosis induction was additionally monitored after H_2O_2 challenge with western blot analysis of cleaved caspase 3 (Figure 3F).

Signs of ER Stress in XP/CS and Analysis of $Csb^{m/m}$ Mice

We next asked whether TUDCA treatment de-represses RNA polymerase I transcription in CS cells resulting in less error-prone ribosomes. We treated CS cells with this chaperone and transfected control and mutant luciferase constructs. As depicted in Figure 4A, TUDCA treatment did not restore translational fidelity of CS cells, indicating that de-repression of RNA polymerase I transcription does not restore the quality of translation of CS-ribosomes.

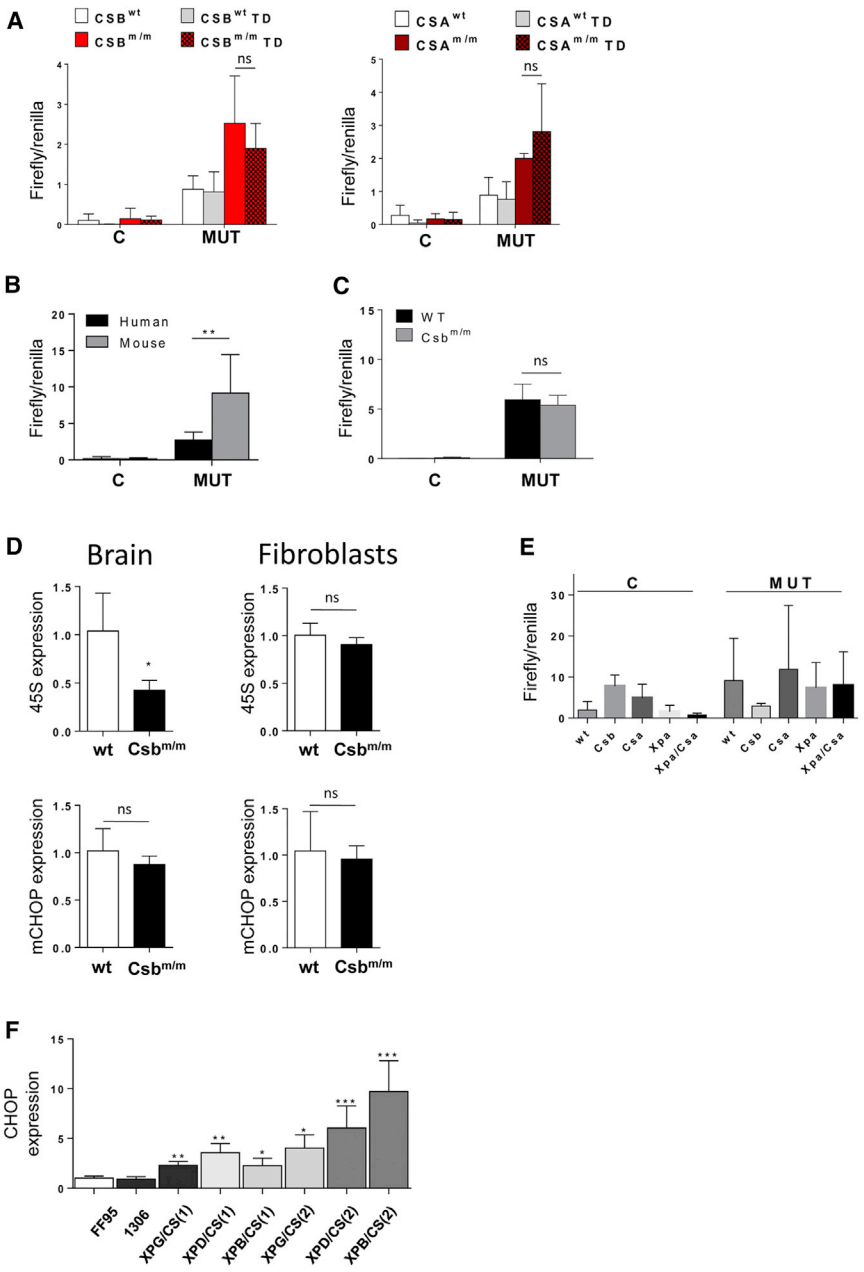

Figure 4. Analysis of Mouse Cells and Signs of ER Stress in XPB, XPD, and XPG Mutant Cells

(A) The effect of TUDCA on translation accuracy was measured in CS and control cells by transfection of control or mutant firefly luciferase reporters with a mutated critical lysine 529, determining the frequency of amino acid misincorporation. The activity of the luciferase was determined by luminescence measurement and normalized to the luminescence of Renilla luciferase. Values are mean ± SD of three independent experiments.

(B) Translation accuracy was measured in wild-type human fibroblasts and in wild-type mouse fibroblasts by transfection of control or mutant firefly luciferase reporters. The activity of the luciferase was normalized to the luminescence of *Renilla* luciferase. Values are mean ± SD of three independent experiments (*$p < 0.05$, **$p < 0.01$).

(C) Translation accuracy in wild-type and Csb mutant mouse fibroblasts. Cells were isolated from 3 wild-type and 3 $Csb^{m/m}$ mice. Values are mean ± SD of three independent experiments.

(D) qPCR analysis of 45S rRNA and CHOP from wild-type and $Csb^{m/m}$ mice. Total RNA was isolated from mouse brain and ear-isolated fibroblasts. Values are mean ± SD of three wild-type and 3 $Csb^{m/m}$ mice (*$p < 0.05$).

(E) Translation accuracy determined in wild-type, $Csb^{m/m}$, $Csa^{m/m}$, $Xpa^{m/m}$, and $Xpa^{m/m}/Csa^{m/m}$ mouse fibroblasts revealed no significant differences. Values are mean ± SD of three independent experiments.

(F) ER stress in XP/CS cells was assessed by expression analysis of ER stress marker CHOP by qPCR. Values are mean ± SD of three independent experiments (*$p < 0.05$, **$p < 0.01$, ***$p < 0.001$).

Next, we compared translational fidelity of human and mouse fibroblasts. The accuracy of wild-type human fibroblasts assessed by luciferase assay was more than 2-fold higher compared to wild-type mouse fibroblasts (Figure 4B). This difference in translational accuracy might contribute to the difference in lifespan between mice and humans.

Subsequently, fibroblasts from mice with the same mutation as the $CSB^{m/m}$ human cells used in this study (van der Horst et al., 1997) were analyzed for signs of impaired translational fidelity. In mice, the mutation of Csb did not affect translational accuracy (Figure 4C). Moreover, although RNA polymerase I transcription was significantly reduced in the brain of mutant mice but not in fibroblasts (Figure 4D), this was not associated with an elevated ER stress or activated UPR. In addition, ROS levels were not increased in $Csb^{m/m}$ mouse fibroblasts (Figure S4A).

Double mutant mice, such as $Xpa^{m/m}$/$Csa^{m/m}$, develop a severe phenotype with premature aging and shortened lifespan (Brace et al., 2013). However, in dermal fibroblasts isolated from these mice, translational fidelity and ROS levels were normal (Figures 4E and S4B).

Finally, we investigated signs of an elevated UPR also in the cells from patients with the rare combined phenotype of Xeroderma pigmentosum (XP) and CS. Cells from these patients showed a reduced RNA polymerase I transcription elongation (Figure S4C). Remarkably, increased p-eIF2α levels (Figure S4D) triggered a high activation of the UPR-specific apoptosis inducer CHOP in XP/CS cells, indicating ER stress (Figure 4F). Our study reveals that loss of proteostasis may represent a previously unrecognized pathomechanism in premature aging or aging itself.

DISCUSSION

Over the past years, we and other groups have identified ribosomal DNA transcription by RNA polymerase I as a common function of the CS proteins. In this study, we investigated the consequences of a malfunction in RNA polymerase I transcription and described how a disturbed ribosomal biogenesis might be linked to growth failure and neurological degeneration in CS.

The slow growth of CS cells can be explained by the reduction in rDNA transcription. Although we detected similar levels of ribosomes in CS and control cells, the synthesis of new ribosomes might be significantly delayed due to reduced rRNA synthesis. Surprisingly, ribosomes from CS cells also exhibited an activity defect, as the translation per ribosome was diminished in CSA and CSB mutant cells. Because both CS features—reduced RNA polymerase I transcription and protein synthesis—could be alleviated by dampening of ER stress by treatment with chaperones, they most likely result from an over-activated UPR. In conclusion, repressed rDNA transcription and translation might contribute to the growth impairment observed in the affected individuals.

To assess the quality of translation in CS cells, we performed a transfection assay that was initially used to detect the elevated translational fidelity of the long-living naked mole rat, *Heterocephalus glaber* (Azpurua et al., 2013). This elevated translational fidelity might contribute to the resistance of proteins to unfolding following urea treatment, described in the naked mole rat cells (Pérez et al., 2009). The resistance of the proteome to unfolding, a feature of the longest-living animal, the sea shell *Arctica islandica* (Treaster et al., 2014), was severely reduced in CS cells, indicating that the amount of misfolded proteins is high. As misfolded proteins are highly susceptible to oxidation (Dukan et al., 2000), and we detected high levels of different ROS species in CS cells, the elevated protein carbonylation in CS cells might be due to the unfortunate combination of both factors. Although the UVs control cells showed the highest levels of ROS, the patient was only mildly affected (Horibata et al., 2004). This indicates that elevated ROS alone do not cause growth defects and premature aging. The UVs control cells reflect the experimental setup recently described (Scheibye-Knudsen et al., 2016), where loss of CSB or CSA was followed by disturbed ribosomal biogenesis, mitochondrial dysfunction, and PARP activation. However, we observed that the total loss of CSB in human cells is not as detrimental as the truncating mutation. Although there are cases of CS patients lacking the CSB protein (Laugel et al., 2008), the discrepancies of these findings and our study require additional investigations.

The high load of misfolded and carbonylated proteins provoked ER stress and UPR as we have shown by elevated GRP78 and p-eIF2α levels in CS cells. P-eIF2α represses overall translation (Wek et al., 2006) and additionally reduces the association of the central RNA polymerase I initiation factor TIF-IA with the rDNA (DuRose et al., 2009). The over-activation of the PERK-eIF2α axis might be the central "suspect" of the mechanism described in this study and has recently been shown to be elevated after CSB knockdown in HeLa cells (Caputo et al., 2017). Additional ER stress, as tested by incubation with tunicamycin, drove CS cells into apoptosis. This could be prevented, similarly to the H_2O_2 hypersensitivity, by addition of chaperones. This supports the hypothesis that these hypersensitivities are mediated by protein oxidation.

Chaperone treatment did not restore translational fidelity of CS cells. They could dampen the ER stress and UPR, but fail to overcome the central problem of the RNA polymerase I transcription, disturbed by mutant CS proteins.

With the same method, we could show that there was a significant difference in translational fidelity between cells of long-living humans and short-living mice. The Csb mutant mice display only a discrete CS phenotype without reduction in growth or lifespan and did not show the herein identified pathomechanism. When additionally to the Csa mutation the central NER factor Xpa is deleted, the mice develop a dramatic premature aging phenotype (Brace et al., 2013). Again, cells of these mice did not display the herein identified pathomechanism, suggesting that the progeria in mice might be mechanistically different.

In summary, we propose that loss of proteostasis may play an important role in CS. Moreover, the administration of pharmaceutical chaperones may dampen the progression of the disease.

EXPERIMENTAL PROCEDURES

Cell Lines

CS1AN and CS3BE cells are SV40-transformed fibroblasts derived from Cockayne syndrome patients. CS1AN carry an A-to-T substitution at nucleotide 1088 (1088A > T) in exon 5 on one allele *ERCC6* (*csb*) gene and a C-to-T substitution at nucleotide 2648 (2648C > T) (Troelstra et al., 1992). CS3BE is an *ERCC8* (*csa*) gene compound heterozygote for mutations at nucleotide 37G > T (E13X) and 479C > T (A160V) (Ridley et al., 2005). Both mutations lead to truncated CSA and CSB proteins. UVSKO SV40-transformed fibroblasts from UVsS patient were used, with a C-to-T homozygous mutation at position 308 of the *ERCC6* (*csb*) gene, generating a stop codon at amino acid position 77 (Horibata et al., 2004). Primary XPD/CS(1)- fibroblasts carrying 1847G > C and 2047C > T mutations and primary XPB/CS(1) (*ERCC3* r.[1010t > a]; [0] c.[1010T > A];[?] p.[Val337Asp]; [0]) fibroblasts were obtained from Vincent Laugel. XPG/CS(1) SV-40 transformed fibroblasts have a homozygous T deletion at position 2972, causing a frameshift after amino acid 925 (Hamel et al., 1996). XPD/CS(2) (GM03248), XPB/CS(2) (GM21072), and XPG/CS(2) (GM16180) human primary fibroblasts were purchased from Coriell Cell Repositores. As controls, stably transfected CS1AN and CS3BE with HA-tagged CSB (HACSB) and CSA (HACSA) proteins were used. Additionally, primary (FF95) and transformed (13O6) human fibroblasts were used as controls. All cells were kept in DMEM (GIBCO) with 10% fetal bovine serum (FBS, Biochrom), 2 mM L-glutamine, 100 U/mL penicillin, and 100 μg/mL streptomycin (all from Merk Millipore). The work with patient's cell lines was approved by the ethical committee of Ulm University (323/16).

Mouse Experiments

In vivo experiments were performed using $Csb^{m/m}$ mice that carry a premature stop codon in exon 5, mimicking the K337stop truncation mutation from the CS1AN patient. The mouse line has been generated and characterized by van der Horst et al. (1997). Although it is considered a null mutant, the expression of an N-terminal CSB fragment cannot be fully excluded. For the experiments, 6-week-old male $Csb^{m/m}$ and wild-type C57BL/6J mice were used. After sacrificing the mice using 5% isoflurane and cervical dislocation, the brain and liver were collected and snap frozen in liquid nitrogen. For primary fibroblasts isolation, skin biopsies from ears were collected, minced, and incubated for 3 hr with collagenase in the cell culture media (DMEM supplemented with 10% FBS, 2 mM L-glutamine, 100 U/mL penicillin, and 100 μg/mL streptomycin). After collagenase dissociation, the cells were centrifuged, incubated

in normal media, and further propagated for the described experiments. Breeding and maintenance of mice was performed at the animal facility of Ulm University under pathogen-free conditions. All experiments were approved by the Regierungspraesidium Tübingen (Z.191).

Antibodies

Antibodies against GRP78 (3177P), Phospho-eIF2α (9721L), eIF2α (9722), CHOP (2895P), and Caspase-3 (9661S), were obtained from Cell Signaling. RPL11 antibody was purchased from Proteintech Europe (16277-1-AP). HRP-coupled β-Actin (sc-1615) from Santa Cruz, and rabbit or mouse secondary antibodies from Dianova.

RNA Extraction and qRT-PCR

Total RNA from exponentially growing CS1AN, CS3BE, UVsKO, HACSB, HACSA, FF95, XPD/CS(1), XPB/CS(1), XPG/CS(1), XPD/CS(2), XPB/CS(2), and XPG/CS(2) was isolated using RNeasy Kit (QIAGEN). 1 μg RNA was reverse transcribed using random primer $p(dN)_6$ (Roche). The expression of 47S precursor rRNA, 18S rRNA, CHOP, ATF6, and ATF4 was quantified by real-time PCR (Applied Biosystems). Data were normalized to the level of RPL13 mRNA.

Ribosome Isolation

The isolation of ribosomes was performed according to the method of Penzo et al. (2015). In summary, 4×10^6 cells were pelleted and lysed adding 2× packed cell volume of 10 mM Tris-HCl, pH 7.4, 10 mM NaCl, 3 mM $MgCl_2$, and 0.5% Nonidet P-40. After 10 min incubation on ice, the lysates were centrifuged at 20,000 × *g* for 10 min at 4°C. The supernatants were collected and ribosomes were pelleted by ultracentrifugation (15 hr at 120,000 × *g*, 4°C) through a discontinuous sucrose gradient consisting of 2.25 mL of 1.0 M sucrose and 2.25 mL of 0.7 M sucrose, both containing 30 mM HEPES/KOH, pH 7.5, 2 mM magnesium acetate, and 1 mM DTT; KCl was 0.5 M in the 0.7 M layer and 70 mM in the 1 M sucrose layer.

Metabolic Labeling

Cells were harvested using Accutase (Sigma) and counted. 5×10^5 cells were starved for 20 min using DMEM/dialyzed FBS lacking methionine/cysteine and subsequently labeled with 35S methionine/cysteine (10 μCi/mL). After 2 hr, incubation media was removed and the reaction was stopped by washing with ice-cold PBS and TCA precipitation for 90 min on ice. Each precipitate was spotted on glass filters, washed, and the incorporated radioactivity was measured in a scintillation counter (Beckman Coulter).

Carbonylation Assay

The concentration of carbonylated proteins was determined using Protein Carbonyls Assay Kit (Abnova). Protein lysates were incubated with 2,4-dinitrophenylhydrazine (DNPH) for 10 min at room temperature and precipitated with TCA (5 min at room temperature). Each sample was centrifuged and the pellets were washed two times with cold acetone. Precipitated proteins were solubilized in 200 μL guanidine, transferred into a 96-well plate, and measured at an optical density of 375 nm. The values were normalized according to the protein content, measured by BCA assay (Thermo Scientific).

ROS Measurement by Fluorescence-Activated Cell Sorting

For ROS detection cells were stained for 15 min with fluorescent dyes dihydroethidium (DHE, 10 μM, Invitrogen) and CM-H_2DCFDA (1 μM, Invitrogen). Cells were then washed with PBS and harvested in 0.5 mL fluorescence-activated cell sorting (FACS) buffer. Fluorescence was measured by FACSCanto II (BD Biosciences) and analyzed using FlowJo software (BD Biosciences).

Proteasome Activity

Proteasomal degradation of proteins was determined using 20S Proteasome Assay Kit (Cayman). SUC-LLVY-AMC 20S substrate was used, which upon cleavage by the active enzyme generates a highly fluorescent product (360 nm excitation, 480 nm emission). 10^5 cells were seeded in a 96-well plate overnight and centrifuged once at 500 × *g*. Cells were washed once with Proteasome Assay Buffer, centrifuged 5 min at 500 × *g*, and incubated 30 min with 100 μL of Proteasome Lysis Buffer. 90 μL of each lysate was incubated with 10 μL of Substrate solution for 1 hr at 37°C, followed by fluorescence measurement using a microplate reader. Jurkat cell lysate supernatants were used as positive controls and 20S Inhibitor Solution was used as negative control.

BisANS

Changes in protein folding and protein stability were tested by staining with fluorescent dye BisANS (Sigma). Cells were harvested in TNE buffer (50 mM Tris HCl, 100 mM NaCl, 1 mM EDTA), sonicated (3 × 30 s) and centrifuged for 20 min at maximum speed. 100 μg of protein from the supernatant was subjected to 2 M urea (final volume of 200 μL) for 2 hr. BisANS was added in each sample (20 μM final concentration) and the fluorescence was measured using an excitation wavelength of 375 nm and 500 nm emission.

Apoptosis (Nicoletti Assay)

Identification of a hypodiploid DNA content of CS, XP, and FF95 fibroblasts after H_2O_2 and tunicamycin treatment was performed as described by Nicoletti et al. (1991).

Transfection and Luciferase Assay

10^6 cells were transfected with Nucleofector transfection (Lonza), using 5 μg reporter plasmid and 0.1 μg *Renilla* luciferase plasmid. Cells were plated in a 96-well plate (5×10^4 cells/well in 75 μL), and allowed to grow for 24 hr. To analyze the transfected cells, a Dual-Glo assay kit (Promega) was used. The ratio of firefly to *Renilla* was calculated and used as an indicator of translational fidelity.

Statistical Analysis

Statistical analysis was calculated using GraphPad Prism (GraphPad 6 software). Each experiment was performed independently at least three times, for each individual experiment using minimum three technical replicates. Data are shown as mean ± SD. Statistical significance was calculated using unpaired two-tailed Student's t test in GraphPad Prism software. Asterisks (*) in the figures represent p values (*$p < 0.05$, **$p < 0.01$, ***$p < 0.001$).

SUPPLEMENTAL INFORMATION

Supplemental Information includes Supplemental Experimental Procedures, four figures, and one table and can be found with this article online at https://doi.org/10.1016/j.celrep.2018.04.041.

ACKNOWLEDGMENTS

We thank Hartmut Geiger for critical comments on the manuscript, Meinhard Wlaschek for crucial discussions, and Zhonghe Ke and the Gorbunova Group of the University of Rochester for the luciferase mutant constructs. We would like to thank James Mitchell for the double mutant mouse cells. The $Csb^{m/m}$ mice were a kind gift from Bernd Epe, CS1AN cells were from Alan Lehmann, and CS3BE, HA-CSA, and HA-CSB cells were from Mark Berneburg. The UVsKO cells were kindly provided by K. Tanaka. This work was supported by the German Research Foundation DFG through the program CEMMA and grants IB83/3-3 to S.I. and ES431/1-1 to P.R.E.

AUTHOR CONTRIBUTIONS

Investigation, M.C.A., P.M., F.T., I.K., M.P., and A.S.; Writing – Original Draft, M.C.A.; Writing – Review & Editing, S.I., I.K., F.T., and R.P.; Conceptualization, S.I.; Funding Acquisition, S.I.; Resources, P.R.E. and V.L.; Supervision, L.M. and K.S.-K.

DECLARATION OF INTERESTS

The authors declare no competing interests.

Received: October 11, 2017
Revised: March 2, 2018
Accepted: April 9, 2018
Published: May 8, 2018

REFERENCES

Assfalg, R., Lebedev, A., Gonzalez, O.G., Schelling, A., Koch, S., and Iben, S. (2012). TFIIH is an elongation factor of RNA polymerase I. Nucleic Acids Res. *40*, 650–659.

Azpurua, J., Ke, Z., Chen, I.X., Zhang, Q., Ermolenko, D.N., Zhang, Z.D., Gorbunova, V., and Seluanov, A. (2013). Naked mole-rat has increased translational fidelity compared with the mouse, as well as a unique 28S ribosomal RNA cleavage. Proc. Natl. Acad. Sci. USA *110*, 17350–17355.

Brace, L.E., Vose, S.C., Vargas, D.F., Zhao, S., Wang, X.P., and Mitchell, J.R. (2013). Lifespan extension by dietary intervention in a mouse model of Cockayne syndrome uncouples early postnatal development from segmental progeria. Aging Cell *12*, 1144–1147.

Bradsher, J., Auriol, J., Proietti de Santis, L., Iben, S., Vonesch, J.L., Grummt, I., and Egly, J.M. (2002). CSB is a component of RNA pol I transcription. Mol. Cell *10*, 819–829.

Brooks, P.J. (2013). Blinded by the UV light: how the focus on transcription-coupled NER has distracted from understanding the mechanisms of Cockayne syndrome neurologic disease. DNA Repair (Amst.) *12*, 656–671.

Caputo, M., Balzerano, A., Arisi, I., D'Onofrio, M., Brandi, R., Bongiorni, S., Brancorsini, S., Frontini, M., and Proietti-De-Santis, L. (2017). CSB ablation induced apoptosis is mediated by increased endoplasmic reticulum stress response. PLoS ONE *12*, e0172399.

Cleaver, J.E., Brennan-Minnella, A.M., Swanson, R.A., Fong, K.W., Chen, J., Chou, K.M., Chen, Y.W., Revet, I., and Bezrookove, V. (2014). Mitochondrial reactive oxygen species are scavenged by Cockayne syndrome B protein in human fibroblasts without nuclear DNA damage. Proc. Natl. Acad. Sci. USA *111*, 13487–13492.

Dukan, S., Farewell, A., Ballesteros, M., Taddei, F., Radman, M., and Nyström, T. (2000). Protein oxidation in response to increased transcriptional or translational errors. Proc. Natl. Acad. Sci. USA *97*, 5746–5749.

DuRose, J.B., Scheuner, D., Kaufman, R.J., Rothblum, L.I., and Niwa, M. (2009). Phosphorylation of eukaryotic translation initiation factor 2alpha coordinates rRNA transcription and translation inhibition during endoplasmic reticulum stress. Mol. Cell. Biol. *29*, 4295–4307.

Hamel, B.C., Raams, A., Schuitema-Dijkstra, A.R., Simons, P., van der Burgt, I., Jaspers, N.G., and Kleijer, W.J. (1996). Xeroderma pigmentosum–Cockayne syndrome complex: a further case. J. Med. Genet. *33*, 607–610.

Henning, K.A., Li, L., Iyer, N., McDaniel, L.D., Reagan, M.S., Legerski, R., Schultz, R.A., Stefanini, M., Lehmann, A.R., Mayne, L.V., and Friedberg, E.C. (1995). The Cockayne syndrome group A gene encodes a WD repeat protein that interacts with CSB protein and a subunit of RNA polymerase II TFIIH. Cell *82*, 555–564.

Horibata, K., Iwamoto, Y., Kuraoka, I., Jaspers, N.G., Kurimasa, A., Oshimura, M., Ichihashi, M., and Tanaka, K. (2004). Complete absence of Cockayne syndrome group B gene product gives rise to UV-sensitive syndrome but not Cockayne syndrome. Proc. Natl. Acad. Sci. USA *101*, 15410–15415.

Iben, S., Tschochner, H., Bier, M., Hoogstraten, D., Hozák, P., Egly, J.M., and Grummt, I. (2002). TFIIH plays an essential role in RNA polymerase I transcription. Cell *109*, 297–306.

Koch, S., Garcia Gonzalez, O., Assfalg, R., Schelling, A., Schäfer, P., Scharffetter-Kochanek, K., and Iben, S. (2014). Cockayne syndrome protein A is a transcription factor of RNA polymerase I and stimulates ribosomal biogenesis and growth. Cell Cycle *13*, 2029–2037.

Laugel, V., Dalloz, C., Stary, A., Cormier-Daire, V., Desguerre, I., Renouil, M., Fourmaintraux, A., Velez-Cruz, R., Egly, J.M., Sarasin, A., and Dollfus, H. (2008). Deletion of 5′ sequences of the CSB gene provides insight into the pathophysiology of Cockayne syndrome. Eur. J. Hum. Genet. *16*, 320–327.

Laugel, V., Dalloz, C., Durand, M., Sauvanaud, F., Kristensen, U., Vincent, M.C., Pasquier, L., Odent, S., Cormier-Daire, V., Gener, B., et al. (2010). Mutation update for the CSB/ERCC6 and CSA/ERCC8 genes involved in Cockayne syndrome. Hum. Mutat. *31*, 113–126.

Lebedev, A., Scharffetter-Kochanek, K., and Iben, S. (2008). Truncated Cockayne syndrome B protein represses elongation by RNA polymerase I. J. Mol. Biol. *382*, 266–274.

Martínez, G., Duran-Aniotz, C., Cabral-Miranda, F., Vivar, J.P., and Hetz, C. (2017). Endoplasmic reticulum proteostasis impairment in aging. Aging Cell *16*, 615–623.

Nicoletti, I., Migliorati, G., Pagliacci, M.C., Grignani, F., and Riccardi, C. (1991). A rapid and simple method for measuring thymocyte apoptosis by propidium iodide staining and flow cytometry. J. Immunol. Methods *139*, 271–279.

Nonnekens, J., Perez-Fernandez, J., Theil, A.F., Gadal, O., Bonnart, C., and Giglia-Mari, G. (2013). Mutations in TFIIH causing trichothiodystrophy are responsible for defects in ribosomal RNA production and processing. Hum. Mol. Genet. *22*, 2881–2893.

Pascucci, B., Lemma, T., Iorio, E., Giovannini, S., Vaz, B., Iavarone, I., Calcagnile, A., Narciso, L., Degan, P., Podo, F., et al. (2012). An altered redox balance mediates the hypersensitivity of Cockayne syndrome primary fibroblasts to oxidative stress. Aging Cell *11*, 520–529.

Penzo, M., Rocchi, L., Brugiere, S., Carnicelli, D., Onofrillo, C., Couté, Y., Brigotti, M., and Montanaro, L. (2015). Human ribosomes from cells with reduced dyskerin levels are intrinsically altered in translation. FASEB J. *29*, 3472–3482.

Pérez, V.I., Buffenstein, R., Masamsetti, V., Leonard, S., Salmon, A.B., Mele, J., Andziak, B., Yang, T., Edrey, Y., Friguet, B., et al. (2009). Protein stability and resistance to oxidative stress are determinants of longevity in the longest-living rodent, the naked mole-rat. Proc. Natl. Acad. Sci. USA *106*, 3059–3064.

Ridley, A.J., Colley, J., Wynford-Thomas, D., and Jones, C.J. (2005). Characterisation of novel mutations in Cockayne syndrome type A and xeroderma pigmentosum group C subjects. J. Hum. Genet. *50*, 151–154.

Scheibye-Knudsen, M., Tseng, A., Borch Jensen, M., Scheibye-Alsing, K., Fang, E.F., Iyama, T., Bharti, S.K., Marosi, K., Froetscher, L., Kassahun, H., et al. (2016). Cockayne syndrome group A and B proteins converge on transcription-linked resolution of non-B DNA. Proc. Natl. Acad. Sci. USA *113*, 12502–12507.

Schmitz, K.M., Schmitt, N., Hoffmann-Rohrer, U., Schäfer, A., Grummt, I., and Mayer, C. (2009). TAF12 recruits Gadd45a and the nucleotide excision repair complex to the promoter of rRNA genes leading to active DNA demethylation. Mol. Cell *33*, 344–353.

Treaster, S.B., Ridgway, I.D., Richardson, C.A., Gaspar, M.B., Chaudhuri, A.R., and Austad, S.N. (2014). Superior proteome stability in the longest lived animal. Age (Dordr.) *36*, 9597.

Troelstra, C., van Gool, A., de Wit, J., Vermeulen, W., Bootsma, D., and Hoeijmakers, J.H. (1992). ERCC6, a member of a subfamily of putative helicases, is involved in Cockayne's syndrome and preferential repair of active genes. Cell *71*, 939–953.

van der Horst, G.T., van Steeg, H., Berg, R.J., van Gool, A.J., de Wit, J., Weeda, G., Morreau, H., Beems, R.B., van Kreijl, C.F., de Gruijl, F.R., et al. (1997). Defective transcription-coupled repair in Cockayne syndrome B mice is associated with skin cancer predisposition. Cell *89*, 425–435.

van der Horst, G.T., Meira, L., Gorgels, T.G., de Wit, J., Velasco-Miguel, S., Richardson, J.A., Kamp, Y., Vreeswijk, M.P., Smit, B., Bootsma, D., et al. (2002). UVB radiation-induced cancer predisposition in Cockayne syndrome group A (Csa) mutant mice. DNA Repair (Amst.) *1*, 143–157.

Wek, R.C., Jiang, H.Y., and Anthony, T.G. (2006). Coping with stress: eIF2 kinases and translational control. Biochem. Soc. Trans. *34*, 7–11.